THERMO-RESPONSIVE BEHAVIOUR OF CELLULOSIC MATERIALS

BŘETISLAV ČEŠEK,[*] MILOSLAV MILICHOVSKÝ,[*] JAN GOJNÝ[*] and DAVID BŘÍZA[**]

[*]*University of Pardubice, Faculty of Chemical Technology, Institute of Chemistry and Technology of Macromolecular Materials, 95, Studentská, 532 10 Pardubice, Czech Republic*
[**]*Huhtamaki Česká Republika, a.s., 675 21 Přibyslavice 101, Czech Republic*

Thermo-responsive hydrated macro-, micro- and submicro-reticular systems, particularly polymers forming hydrogels or similar networks, have attracted extensive interest as they comprise biomaterials, smart or intelligent materials. Phase transition temperature (low or upper critical solution temperature) of the thermo-responsive hydrated reticular systems, which exhibit a unique hydration-dehydration change, is a typical characteristic.
The macro-reticular systems with weak bonding are represented by papermaking pulp slurries composed of cellulosic or ligno-cellulosic fibres.
During wet pulp beating, it was found that the characteristic decrease of the pulp drainability with increasing the input of beating energy abruptly enhanced if the temperature of the beating pulp slurry was higher than 40 °C. Similar observations have been made during pulp slurry drainage at higher temperatures. The drainability of pulp slurries not only improves at temperatures higher than 40 °C, but also it tends to be higher than that obtained when decreasing water viscosity only.

Keywords: thermo-responsive hydrated system, hydrogel, phase transition temperature, beating, drainability

INTRODUCTION

Stimuli-responsive polymers (so-called smart polymers) have recently attracted great interest in academic and applied science. The most common approach takes advantage of thermally induced, reversible phase transitions. In this context, polymers forming hydrated reticular systems found great interest. Hydrated reticular systems, i.e. networks in water environment, characterise all bioentities and the products of their existence. We can identify these structures in submicro-scale, micro-scale and macro-scale as submicro-, micro- and macro-reticular hydrated systems.[1] Supramolecular and hypermolecular structures are typical, e.g. the hydrogels on peptide basis and fibre-networks on cellulosic basis.

Hydrogels consist of elastic networks that can uptake as much as 90-99% (w/w) of water in their interstitial space. Hydrogels have high water content and a soft and rubbery consistency. Such systems have been especially focused upon in the biomedical area as they provide an adequate, semiwet three-dimensional environment for cells and tissue interaction and can be combined with biological or therapeutic molecules. They can be also chemically controlled and designed to tailor their mechanical and functional properties.[2-4] Therefore hydrogels have been proposed for a series of biomedical and biological applications, including tissue engineering,[4-5] drug release systems,[6-10] biological sensors,[13-14] temperature and light-responsive films[15] or tuneable hydrogel photonic crystals as optical sensors.[16] The most common hydrogels are the ones obtained by chemical crosslinking of hydrophilic macromolecules. Such linkages prevent the dissolution of the material, but water can penetrate within the structure, causing the swelling of the structure without disrupting the mechanical and geometrical integrity of the structure. If the macromolecules composing the network react to some external variable, e.g. temperature, switching between a stretched to a squeezed state, then the corresponding hydrogel could reversibly swell and deswell in response to this stimulus. Such smart hydrogels have been proposed for a series of biomedical applications,[17-18] not only in the delivery of therapeutic agents,[6-10] but also in tissue engineering,[11-12] intelligent microfluidic switching,[19-21] sensors/diagnostic devices[22-23] and actuators.[24-25]

The most peculiar property of these systems, however, is probably their stimuli-responsive behaviour. The thermo-responsive behaviour is

typical but only of hydrogels, because fibre-networks are composed of high consistency hydrogel fibres distributed in the macro-space of water environment. Thermo-responsive hydrogels undergo a phase transition in response to temperature changes. Up to now, almost all of the thermo-responsive hydrogels have been featured with negatively thermo-responsive volume phase transition, i.e. with the existence of a lower-critical solution temperature (LCST). Below LCST, the un-crosslinked polymer chains are soluble in water, whereas above LCST the polymer chains form submicro- and micro-aggregates, which separate from the solution. Above LCST, the polymer starts a complex self-assembling process, which leads to an aggregation of polymer chains, initially forming nano- and micro-particles, which segregate from the solution.[26] Below the LCST, the crosslinked hydrogel is swollen and absorbs a significant amount of water, whereas above LCST, the hydrogel dramatically releases free water and begins to shrink. Thermo-responsive hydrogels composed of crosslinked polymer chains undergo fast,[27-28] reversible structural changes from a swollen to a collapsed state by expulsing water. However, another kind of thermo-responsive hydrogels also exist, opposite to LCST-hydrogels, i.e. hydrogels with an upper-critical solution temperature (UCST). These hydrogels shrink at lower temperature and swell at higher temperature. The behaviour of such basic linear macromolecules is schematically presented in Fig. 1.

Poly(N-isopropylacrylamide) (PNIPAAm) has been the most widely used macromolecule in thermo-responsive hydrogels with characteristic LCST. Above the LCTS, at around 32 °C in pure water,[4,14-15,28-30] a reversible structural transition occurs from the expanded coil (soluble chains) to compact globules (insoluble state). N,N´-methylenebisacrylamide (MBA) is often utilized as crosslinker.[27,31] Such macromolecular design widens the applicability of such systems in a variety of biomedical applications, including biomineralization on biodegradable substrates.[32] Such modifications are particularly important to tailor the LCST of PNIPAAm-based systems. Recently, a self-oscilating system of hydrogel particles rhythmically changing its volume was described. This system is based on PNIPAAm, MBA and covalently immobilised $Ru^{2+/3+}$ – redox system utilizing the so-called Belousov-Zhabotinsky oscillating reaction.[33]

The UCST hydrogels are mainly composed of an interpenetrating polymer network (IPN) of polyacrylamide (PAAm) and poly(acrylic acid) (PAAc) or poly(acrylamide-co-butyl methacrylate) crosslinked with MBA.[31] The formation of helices (double or triple in polysaccharides, such as agarose, amylase, cellulose derivatives and carrageenans or in gelatine, respectively) and the corresponding aggregation upon cooling, forming physical junctions, are based on hydrogel formation.[17] Dilutable but coacervating quasi-hydrogel with UCST are represented by urea-formaldehyde (UF) pre-condensates.[35-36]

According to the behaviour of thermo-responsive hydrated reticular systems (TRHRS) during dilution,[1] we can divide them into water dilutable and nondilutable, crosslinked 3D networks or crosslinked 2D networks – films. Additionally, it is possible to divide the dilutable TRHRS into fully dilutable polymer solutions at T < LCST (or T > UCST), and coacervated[34-36] submicro- or microTRHRS or flocculated macroTRHRS.
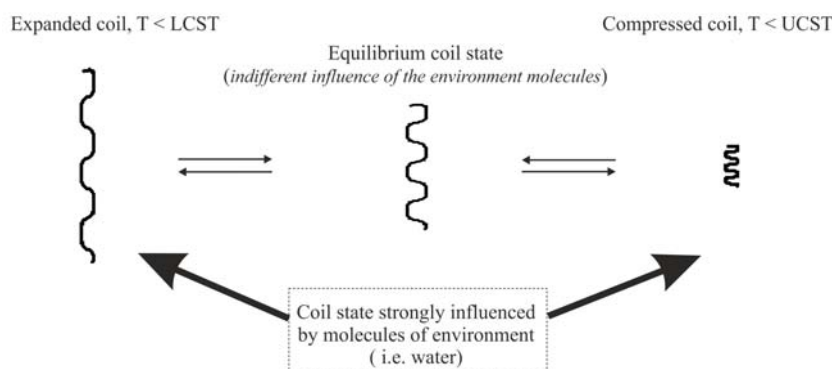

Figure 1: Schematic 2D illustration of linear macromolecule behaviour in hydrated micro- and nano-reticular systems with LCST or UCST

The dilutable[1] TRHRS coacervate or flocculate in a water environment due to the weak bonds among the polymer chains, microparticles and hydrogel particles or fibres and microfibres, respectively. This is typical of the submicro-, micro- and macro-networks that are disrupted during the dilution process, i.e., quasi-hydrogels coacervate and fibre networks flocculate, respectively. As the temperature changes, the sol-gel transition occurs in reversible hydrogels due to non-chemical crosslinks being formed among the grafted and branched elements of the copolymers.

The crosslinked structures created by particularly strong chemical bonds among the polymer chains, like micro- and macro-sponges, have been then swelled or shrunk in response to the temperature change over the LCST. During a volume transition, the hydrogel bonding or anti-bonding system formed between water molecules and the polymeric chains is disturbed, this being thermodynamically favourable to decreasing or increasing in entropy the main driving force for the occurrence of the transition, respectively.

We can conclude[1] that under regular conditions, i.e. at room temperature and inert environment, the PNIPAAm polymer has preferred the thermodynamically advantageous coil conformation, because of the hydrophobic interactions among isopropyl pendant groups. However, due to peculiar water activity, the coil conformation is stretched at a temperature below the LCST, in contradiction with the squeezed original coil conformation above the LCST as the repulsive domain activity is weakened – see schematic illustration in Fig. 1. The peculiar water activity is accompanied below the LCST by the origination of repulsive water action among the polymer chains, its segments, submicro- and micro-colloidal particles etc. arising from equal water molecule orientations at interacting interface microdomains, due to hetero- followed by homo-H-bonds among them, i.e. a hydration anti-bonding system. Obviously, the width of vicinal immobilised water within interacting polymer interfaces decreases with the increase of polymer concentration, because the disruption action of the hydration repulsive forces is weakened dramatically with a temperature increase. As a result, the LCST decreases with polymer concentration increase.[11] Under regular conditions, i.e. at room temperature and inert environment, the UCST hydrated crosslinked and un-crosslinked polymers have preferred the

thermodynamically advantageous long-chain structure, which is squeezed in a water environment to a compressed coil conformation, due to the origination of a weak hydration bonding system. The hydration bonding system[1,35-37] among polymer chains, its segments, submicro- and microcolloidal particles etc. arises from opposite water molecules orientations at the interacting interface microdomains, because of the hetero-H-bonds of the proton-acceptor or proton-donor groups of the polymer chains and homo-H-bonds among water molecules. As the temperature increases, the hydration bonding system is weakened because of the increase in the kinetic energy of water molecules. Above the UCST, the hydration bonding system is weaker than the inner opposite stress of the compressed polymer chains of the TRHRS and the polymer chains expand. As a result, the crosslinked TRHRS swell and the polymer chains in the noncrosslinked TRHRS are dissolved. Below the UCST, the hydration bonding system is stronger than the inner opposite tension of the compressed flexible polymer chains and the long chains of the polymer compress. The process results in deswelling and coacervating of the crosslinked hydrogel and dissolved polymers, respectively. Obviously, the intrahydration bonds squeeze the long-chain uncrosslinked polymer structure into a compressed coil conformation, and the interhydration bonds squeeze the long-chain crosslinked structures to a deswollen form at temperatures below the UCST. However, a different characteristic behaviour is observed if a hydrated reticular system is composed of relatively rigid rod-like particles, such as short polymer chains or fibres. The short polymer chains or fibres in hydrated submicro- or macro-reticular systems, respectively, are formed through interhydration bonds and the interhydration repulsive domains, i.e. mutually functioning hydration bonding and debonding sites. As typical, due to increased fluctuation of the bonding and debonding activities of the interacting microsites during dilution, the submicro-reticular systems coacervate and the macroreticular systems flocculate. The submicro weak bonding of the hydroreticular system, accompanied by coacervation during dilution, is well demonstrated by use of UF precondensate.[1,35-36]

The macro-reticular systems with a weak bonding system are represented by papermaking pulp slurries composed of fibres of cellulosic or

ligno-cellulosic character. It is typical of components with marked papermaking properties that form a fibre network, which is only compressed during sedimentation. This behaviour is called rheosedimentation.[38-39] The basic condition of rheosedimentation is the ability of the pulp fibre to form a network displaying special behaviour, i.e., due to a weak bonding system, the fibre network is compressed by gravity.[39-41] The homogeneous pulp fibre network is formed at a concentration higher than 1 kg/m³ of suspension. The dilution of the suspension under the concentration of 1 g/L is then accompanied by flocculation and rheosedimentation. However, the rheosedimented fibre network is not in a fully homogeneous state, because of the lack of shear forces (agitation) disturbing the rheosedimenting floccules.

Influence of temperature on the behaviour of pulp suspension

The temperature influences both the macro-reticular fibre system and the hydrogel structure of fibres with complex morphology. Predominantly, the temperature-responsive activity of hydrated microstructure of fibres is important from a practical point of view.[1]

The hydration bonding concept, i.e. the formation of hydration weak bonds or antibonds, follows up the SCHL (structural changes in hydration layers) theory.[42] The idea of the origins and effect of hydration forces is based on the typical dipole character of water molecules and on their two possible basic orientations in the hydration spheres (termed as immobilised or vicinal water) around the hydrophilic submicro-domains,[35-37] depending upon their nature.
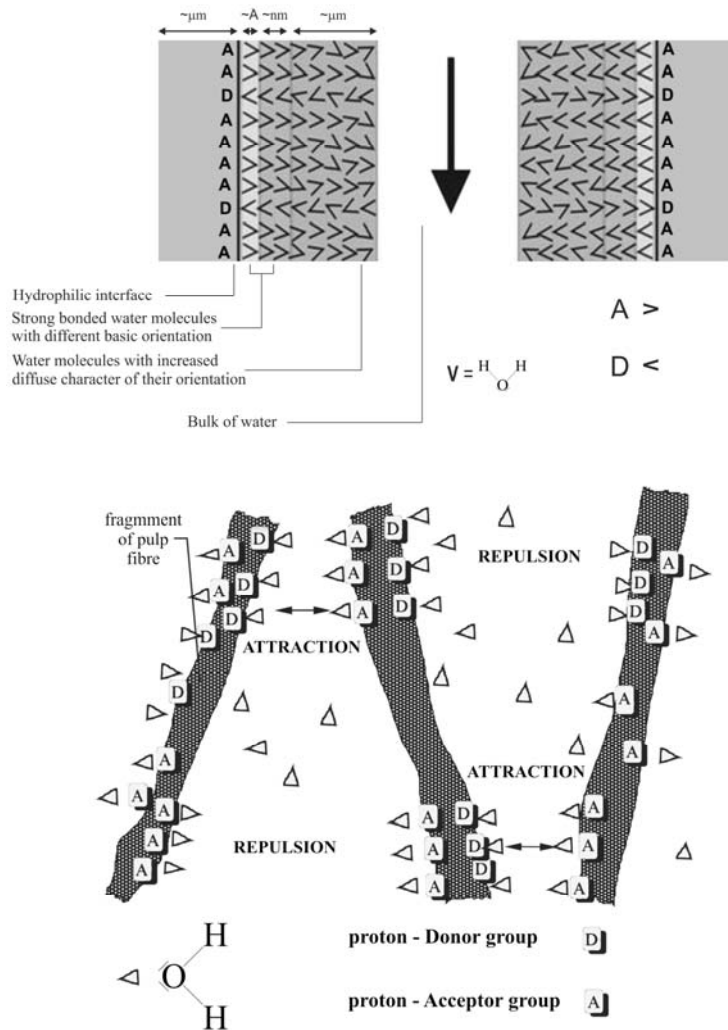

Figure 2: Schematic representation of origin and action of repulsive and attractive hydration forces during the wet-web formation among cellulosic fibre components in water

The possible orientations of water molecules with regard to the hydrophilic domains forming the hydrophilic phase interface vary essentially between the following extreme positions (see Fig. 2):

– ◄ basic orientation with the H-atoms of water molecules to the submicro-domain with proton acceptor activities;

– ► basic orientation with the O-atoms of water molecules to the submicro-domain with proton donor activities.

This difference appears in the interactions of heterogeneous mosaic surfaces[42] containing submicro-domains, in which repulsive and attractive hydration forces act simultaneously, as a kind of equilibrium is established, in which the two interacting surfaces reach a definite optimum distance from each other (see Fig. 2). During the interaction, a mutual diffusion of the hydration spheres takes place, connected with a change of their structure. The effects of the hydration forces decrease with a temperature increase, and practically disappear at the boiling point of water. The structural changes take place on the molecular level, being accompanied by appropriate heat effects.[35-37,42] Theoretically,[42] it has been shown and confirmed experimentally[35] that the action of attractive forces is an exothermic process connected with decreasing entropy, while the action of repulsive hydration forces (i.e. under the influence of external forces) has an endothermic character connected with increasing entropy.

Moreover, the SCHL theory predicts and experiments support the fact that the density of immobilised water is higher than the density of bulk water, in dependence on its vicinity to the hydrophilic domain interface. With increasing distance from the domain interface, the density of water decreases. The difference[43] between vicinal and bulk water is changed in the range of 2 to 40%. Besides this, an important implication that can be derived from here is that the density of water, comparatively to the bulk of water, located between interacting hydrophilic surfaces is higher in the case of attractive hydration forces and lower in the case of repulsive ones.

Influence of temperature on the dewatering process

Filtration is characterized by the flow of liquid through a porous baffle bed. Provided the laminar nature of the flow, Q, in the case of filtering the suspension under normal operating conditions, is met by neglecting the resistance of the filter septum; Darcy's equation is used to describe this process in the form:

$$Q = \frac{dV}{d\tau} = \varepsilon \cdot \frac{S \cdot \Delta p}{L \cdot \mu} \qquad [m^3/s] \qquad (1)$$

where ε is the coefficient of permeability [m^2], dependent on the characteristics of the filter septum with a flat area S [m^2], μ is the viscosity coefficient of dewatered liquid [Pa.s], Δp – the pressure difference [Pa] and L – the height of forming porous bed [m]. However, a wet paper web is usually created from a heterogeneous compressible suspension of pulp[44] governed by a more general relation, like Darcy's equation (2):

$$Q = \frac{dV}{d\tau} = \varepsilon^m \cdot \frac{S \cdot \Delta p}{L^n \cdot \mu} \qquad (2)$$

where m is the empirical constant. The dimensional analysis of this equation gives the expression:

$$m = \frac{n+1}{2} \qquad (2')$$

The coefficient of uniformity, n, is related to the homogeneity of the drained paper sheet. According to the regime of drainage, the coefficient of uniformity shall take different values:

- $n = 1$ – a typical drainage process of homogeneous fibre suspension by the filtration mechanism under static conditions of drainage;

- $n < 1$ – the drainage resistance of a paper sheet rises more slowly than it should. It concerns the creation of filter cakes from the heterogeneous suspension by the percolation mechanism under static conditions of drainage;

- $n > 1$ – the resistance of a paper sheet rises faster than is obtained for a typical filtering process of fibre slurry composed from a homogeneous suspension. It concerns the creation of filter cakes from a heterogeneous suspension under static conditions of a filter process by both the filtration and the percolation mechanisms, in the case of fast sedimentation coarse shares of pulp generate a netting;

- $n = 0$ – the resistance of a paper sheet in the course of drainage does not change at all. It occurs when creating the filter cake from the homogeneous suspension by the

filtration mechanism for dynamic drainage conditions;

- $n < 0$ – the resistance of a paper sheet decreases with the order of the drainage process. It occurs when the creation of the filter cake takes place from a heterogeneous suspension by both the filtration and percolation mechanisms, under dynamic intensive drainage conditions eliminating the fine pulp shares from the filter cake.

Under comparable conditions, dividing Darcy's equations (2) for the two different temperatures, T_1 and T_2, a theoretical relationship (3) was received, which describes the effect of temperature on the drainage velocity during paper sheet preparation.

$$\frac{Q_{T2}}{Q_{T1}} \cdot \frac{\mu_{T2}}{\mu_{T1}} = const. = k \qquad (3)$$

In this respect, it is evident that the change of drainage velocity with the temperature of drained cakes theoretically depends only on the viscosity of the liquid at a given temperature. Since for most liquids, the viscosity decreases with the increasing temperature, it is preferable to filter the warmed suspension. If the drainage of a pulp slurry depends only on the viscosity of water, then the value of parameter k should be independent of temperature.

EXPERIMENTAL
Materials
Ligno-cellulosic fibrous materials of different purity and character were used for beating and drainage experiments. As typical cellulosic fibrous material, primary bleached spruce sulphite pulp was used, VIAN brand-name, from Paskov, Czech Republic, and non-bleached virgin (never dried) hemp pulp, prepared by the alkaline cooking method in OP Papírna s.r.o. (Delfortgroup AG) Olšany, Czech Republic. Air dried spruce stone groundwood represents a typical ligno-cellulosic fibrous material of high lignin content. Recycled fibrous material is represented by grey secondary fibre. Both fibrous materials were prepared at Huhtamaki Přibyslavice, Czech Republic.

The composition of grey secondary fibre:
- – 60% newspapers,
- – 20% magazines,
- – 10% waste corrugated board,
- – 10% non-sorted waste paper.

The above-mentioned materials were mechanically disintegrated in an air-dried state, followed by dipping in tap water for 10 hours. Refining was realised in a laboratory Hollander, at a consistency of approx. 3%, followed by exact measurements of consistency, degree of beating, according to Schopper-Riegler, and pH of the pulp slurry.

Apparatus
The beating device is composed of a conical beating machine, equipped with independent compelled recirculation, cooling loop and electric power measuring set.

The drainage experiments were performed in an apparatus whose design is schematically presented in Figs. 3 and 4. Before the experiments, both the pulp slurry and the drainage device were adjusted to the prescribed temperature.

Measurements
The non-bleached hemp pulp was beaten under laboratory conditions (3% consistency) during 49 minutes at approximately constant operating edge load of the conical beater. The electrical energy consumption was measured and the temperature of the beaten pulp slurry was controlled by independent cooling equipment. The effective beating energy in kWh/kg of oven dried pulp fibre was then recalculated. The degree of beating was expressed according to Schopper-Riegler (in accordance with ČSN EN ISO 5267-1).

Individual drainage measurements were carried out under vacuum in the range of approximately 60 to 83 kPa. Pulp slurries were measured at temperatures of 20, 40, 60 and 70 °C. At the temperature of 20 °C, 11 measurements were carried out at different pressure. For higher temperature, the measurement was carried out at larger intervals of vacuum, depending on the temperature and the change of dry solids of the generated fibrous cakes. Apparatus vacuum was adjusted by the use of a vacuum regulator and its exact value was established on a mercury U-manometer. Each substance was diluted before the beginning of the measurement, so that the resulting filter cake was prepared from 500 ml pulp suspension and its grammage was approximately 400 g/m².

The received data of dry matter contents were verified by the use of empirical functions as follows:

$$C(T) = C_0(T) + a(T) \cdot \Delta p^{b(T)} \qquad (4)$$

where C_0 is dry matter content of the created filter cake under zero vacuum, Δp is a vacuum, a and b are empirical parameters (depending on temperature T).

Some of these functions are presented in Fig. 6. All measurements were performed at least three times, and the data were in good agreement within a deviation of 2%.
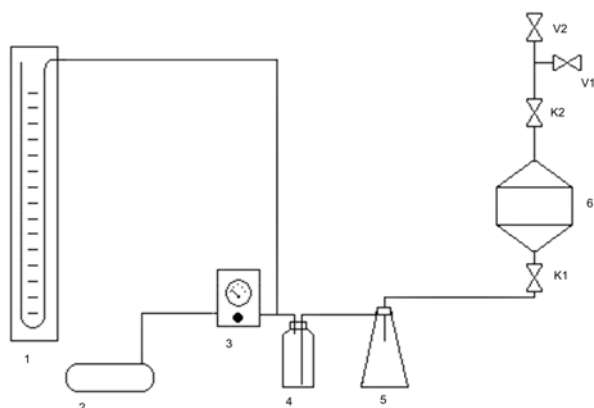
Figure 3: Scheme of drainage apparatus; 1 – U-manometer, 2 – vacuum pump, 3 – vacuum regulator, 4 – washing flask, 5 – vacuum flask, 6 – drainage device, K1, K2 – taps, V1, V2 – valves
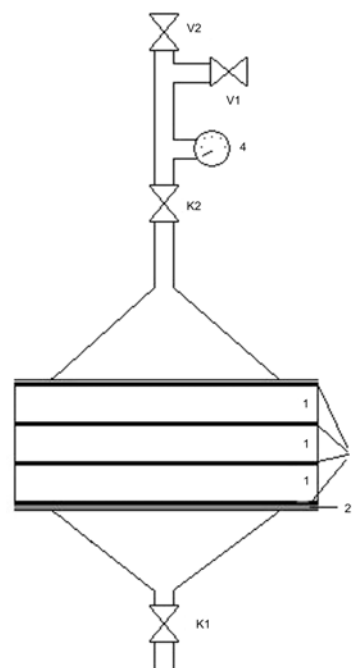

Figure 4: Scheme of drainage device; 1 – plastic annulus, 2 – wire with a rubber seal, 3 – rubber gasket, 4 – pressure gauge

RESULTS AND DISCUSSION

As demonstrated by Fig. 5, the temperature influences both the macro-reticular fibre system and the hydrogel structure of fibres with complex morphology. Predominantly, the temperature-responsive activity of the hydrated microstructure of fibres is important from a practical point of view. We have observed during wet pulp beating that the characteristic decrease of pulp drainability with increasing input beating energy is abruptly increased if the temperature of the beating pulp slurry is higher than 40 °C – see Fig. 5. This fact indicates some LCST behaviour of the hydrogels forming the walls of beaten fibres. Contrary to the swelled state below the LCST, as the temperature is raised above the LCST the fibre hydrogels shrink, i.e. at a temperature above the LCST of fibres, the pulp slurry is better drained and vice versa.

The impact of the temperature of dewatered paper suspension on its drainability and dry matter content of paper sheets was monitored at various vacuums. As follows from Fig. 6, the dry matter content increases with temperature. Furthermore, it has been indicated that the dry matter content of filter cakes increases with the growth of vacuum (pressure difference),

depending on the composition of dewatered pulp. For example, the dry matter of the filter cake consisting of sulphite bleached pulp increases almost linearly with the increase of vacuum. On the other hand, in the case of the grey secondary fibre, the dry matter content increases exponentially with the increase of vacuum. At first sight, the dryness increase of the drained paper sheet with temperature can be explained by certain LCST behaviour of the hydrogels forming the walls of ligno-cellulosic fibres. As expected, primary fibres (especially groundwood) are more sensitive to temperature than secondary ones.

It appears that parameter k, describing relative drainage velocity, is not invariant with respect to temperature, with the increase of temperature it drops – see Fig. 7. This means that with the growth of temperature the drainability of fibrous pulp-based beds is increased, but not so as to match the decline in the viscosity of water with the temperature. The resulting decrease in drainage velocity is even greater than the decrease in water viscosity. Should k be constant, the drainability under various temperatures would be dependent only on the change of liquid viscosity (in this case, water) with the temperature (see Eq. 3).
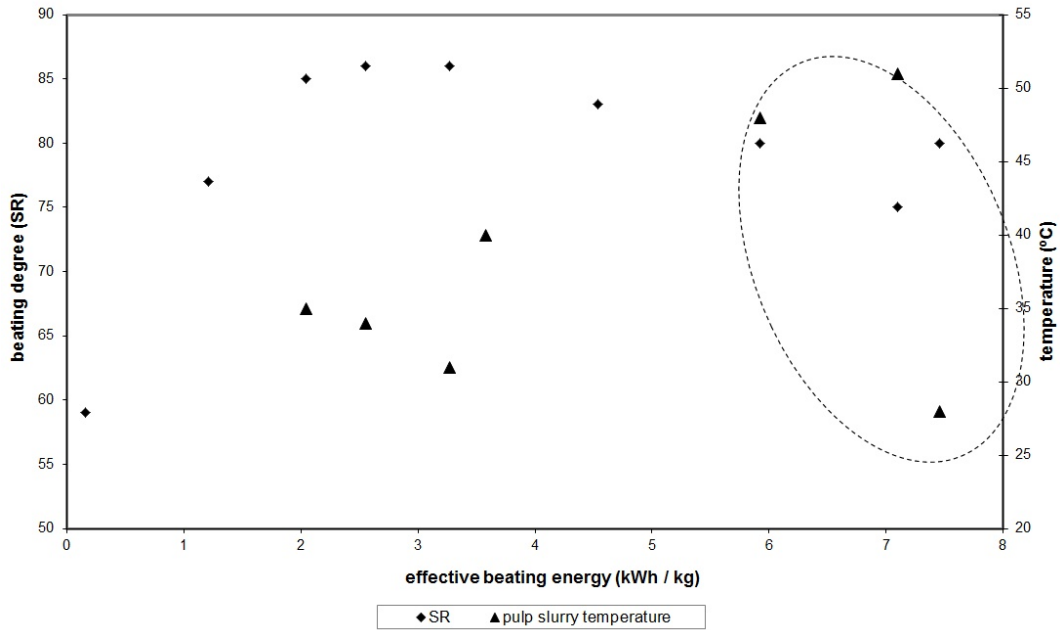
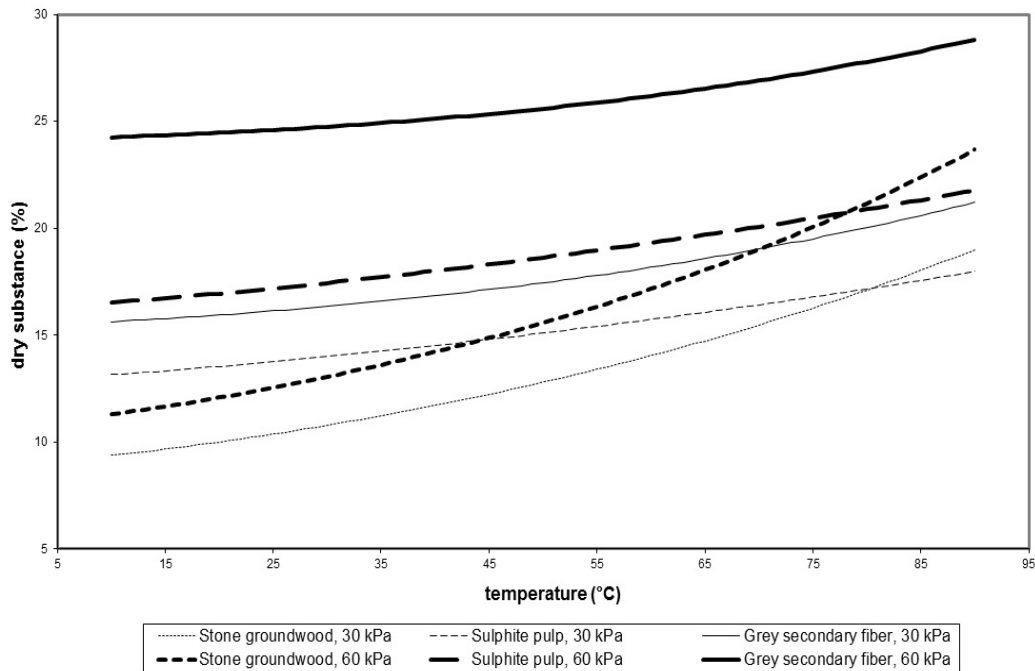Figure 5: Temperature of pulp slurry influence upon drainability of beaten hemp pulp

Figure 6: Dryness of dewatered fibre cake vs. temperature at two different pressures

The observed phenomenon of decrease in the drainability of filter cakes with the increase of temperature can be explained by the SCHL theory – see Fig. 8. This decline, however, similar to the dependencies of the dry matter on the temperature, varies with the composition of pulp. A greater decrease of k with temperature occurs in the case of both virgin and primary fibres, compared to secondary fibres. Interestingly, in the case of the primary fibres, the high-yield ligno-cellulosic mechanical pulp (stone groundwood) practically does not differ from the low-yield ligno-cellulosic chemical pulp (bleached sulphite pulp).

Explanation of this behaviour by the SCHL theory

The water in the pores, lumen etc., but always around the microinterfaces of the pulp fibres forming porous fibrous cakes, is the so-called immobilized layer of water, which is formed by vicinal water having theoretically infinite viscosity in the immediate proximity of this interface (see Fig. 8). Between these immobilized layers inside of the liquid is then the mobile water having a viscosity corresponding to a given temperature. The interface between the immobilized and run-off water from the pore is not exactly defined, but has a transitional viscosity character of digressive nature – its thickness depends on the velocity gradient, i.e. shear rate. The greater is the velocity gradient under comparable conditions, the smaller is the thickness of the immobilized water and vice versa. Moreover, the behaviour of the flowing water between the walls of the pores is then determined by the nature of water molecules orientation in the immobilized microlayers.[37]

If this arrangement of water molecules in the immobilised water microlayers of opposite sites of pores is the same, then the mutual interactions of water molecules are characterized by repulsive hydration forces. Additionally, the result of these interactions is an increasing mobility of water molecules in these microlayers, facilitating the drainabilities of the fibrous bed, because the immobilised water layers have become thinner. On the contrary, if this arrangement of water molecules in the immobilised water microlayers of opposed sites of pores is the opposite, i.e. water molecules are more ordered and more oriented in the micro-domains of immobilized water shells due to the operated attractive hydration forces, the growth in the thickness of the immobilized water is characteristic. Such behaviour results in the thinning of the flow cross section of the pores and hence the drainability of the fibrous bed slows down (see Fig. 9).

The increase of water molecules movement with the increase of temperature leads to reducing its viscosity and of the shell of immobilised pore water, but a bulk of mobilised pore water extends to larger distances. Under comparable conditions, this is reflected by an increase in the dry matter content and the improved drainability of the dewatered fibrous cake.
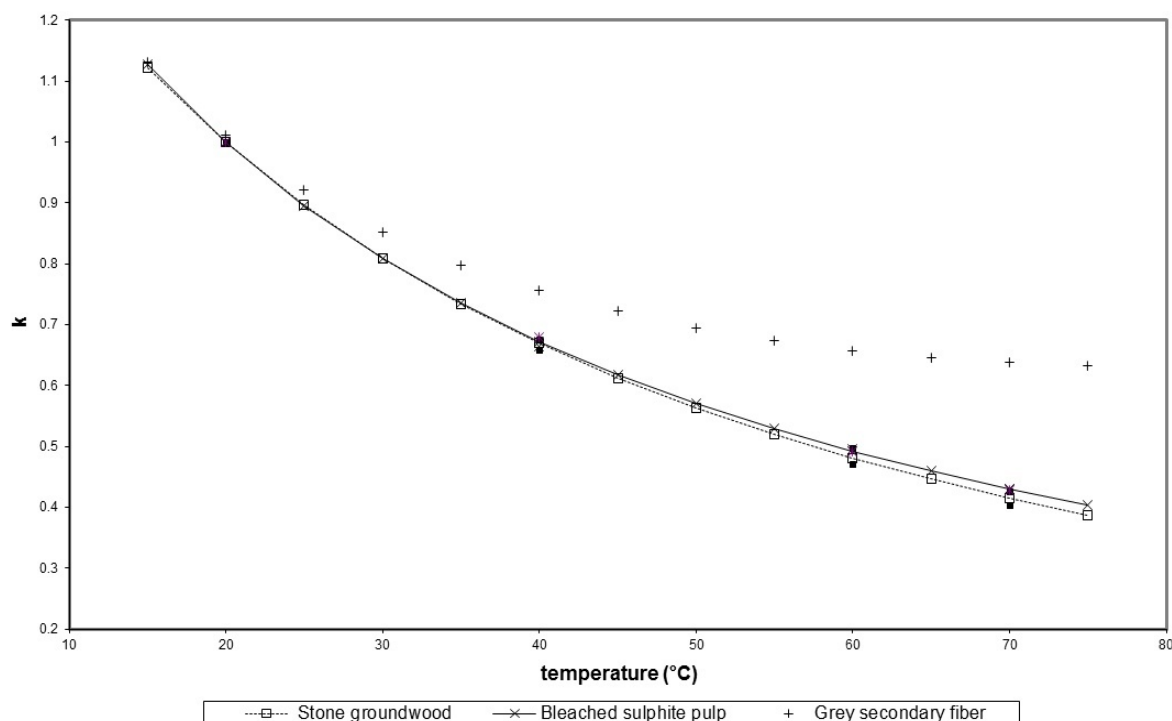

Figure 7: Temperature dependence of parameter k for different fibres (drained at a pressure of 60 kPa, approximately)
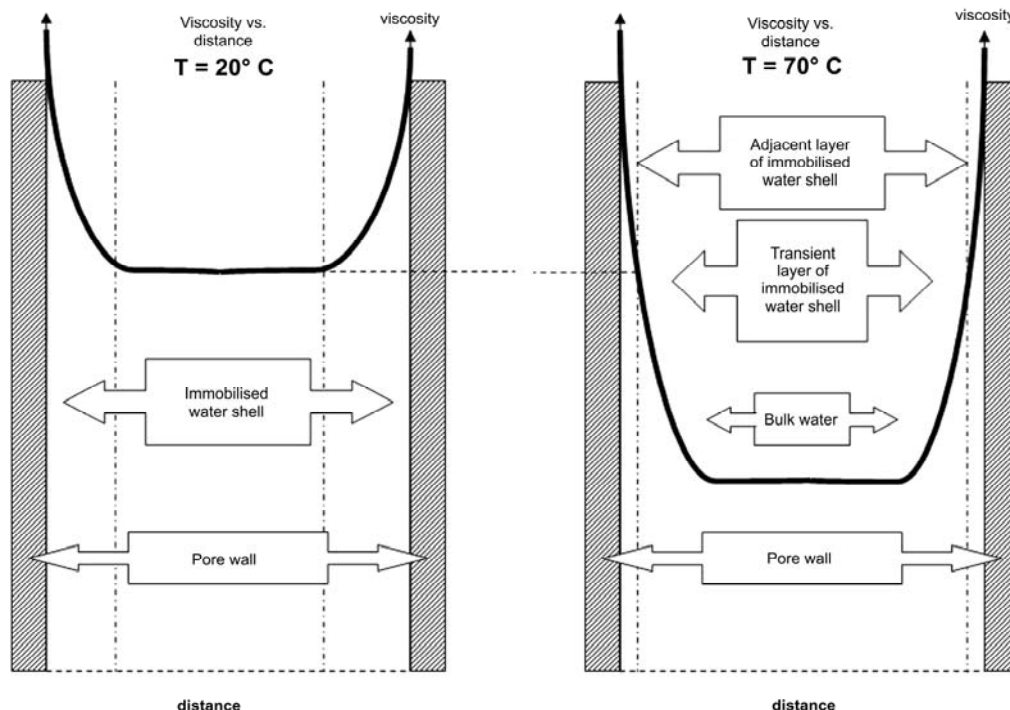
Figure 8: Schematic representation of water viscosity distribution via pore walls, as a function of temperature, resulting in increasing of dry matter and decreasing drainability of paper sheets
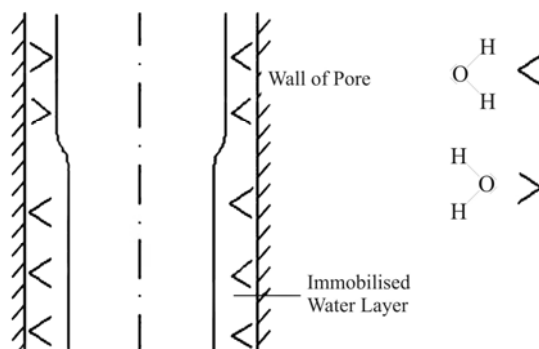

Figure 9: Schematic representation of the influence of water molecules orientation upon the width of pore immobilised water layer

As shown in Fig. 8, with the increase of temperature, the immobilised water does not disappear, but only reduces its viscosity and the thickness of the transient part of the immobilised water shell expands. The part of the immobilized layer with the same water viscosity as at a lower temperature is only reduced. The rest of immobilized water has only a lower viscosity, but still higher than the viscosity of the internal bulk of water. The thickness of the transient nanolayer varies with the viscosity depending on temperature, and as already noted, it has been increasing. This effect causes a relative decrease of the drainage velocity of the ligno-cellulosic fibrous cake with the growth of temperature. By the influence of the increased temperatures, both

the viscosity of the bulk water and the immobilized water will relatively reduce, but the section with the bulk of water decreases also (see Fig. 8). This phenomenon will hinder the flow of water situated in the nanolayers, forming the transition between the immobilised and the normal bulk of water, which affects negatively the overall outflow of water from the fibrous cake.

The overall result is that, due to the growth of temperature, the apparent diameter of the pores is increased, but does not increase to such an extent of drainage velocity, as to correspond to the decrease of normal water viscosity, because of the existing transient immobilised water layers around the pores. To be noted that transient immobilised water is distinguished by a higher

viscosity than the bulk of water. This transition state of immobilised water then slows down all water flowing out from the fibrous bed.

CONCLUSION

Temperature influence on the behaviour of a ligno-cellulosic fibrous slurry was monitored. It was confirmed that with increasing temperature, the dry matter content of the filter cakes, as well as the drainability of fibrous slurries, increased. The hydrated ligno-cellulosic matter behaved as a hydrocolloid with characteristic LCST of approximately 40 °C. However, the dewatered fibrous bed behaviour was not as simple as it was observed from water viscosity changes with temperature. The drainability of real ligno-cellulosic fibrous slurries increased with increasing the temperature, but to a smaller extent than it could be inferred from the water viscosity decrease. This is explained by the more complex behaviour of the ligno-cellulosic fibrous slurry during its drainage as a function of temperature.

The presented explanation is based on the concept of attractive and repulsive hydration forces acting among the pores of the dewatered ligno-cellulosic fibrous bed and being strongly influenced by temperature. Immobilised water shells around the pore walls are composed of oriented water molecules mutually influencing themselves in opposite sites of the pores, thus creating microdomains with attractive or repulsive hydration forces. With the increase of temperature, the action of hydration forces is weakened, i.e. the width of immobilised water layers decreases. This decrease does not change abruptly, it continues across vicinal water shells, thus representing a transient part of the immobilised water shells. This effect then results in slowing down the drainage of the fibrous bed.

We can conclude that the water inside the pores of a ligno-cellulosic material is composed physically by three sorts of water:

- non-moveable adjacent part of immobilised water shell with the highest viscosity at a given temperature and flow conditions;
- transient part of immobilised water shell, flowing with higher viscosity at a given temperature and flow conditions;
- bulk water in the middle of the pores, flowing with a normal viscosity coefficient at a given temperature.

SYMBOLS

T temperature [°C]
Q flow [m^3/s]
S area [m^2]
Δp pressure difference [Pa]
L height of forming porous bed [m]
m empirical constant Eq. (2) [-]
n coefficient of uniformity Eq. (2) [-]
k parameter Eq. (3) [-]
$C(T)$ dry matter content of created filter cake for given temperature T [%]
$C_0(T)$ dry matter content of created filter cake under zero of the vacuum for given temperature T [%]
a, b empirical parameters in Eq. (4) [-]

Greek Letters

ε coefficient of permeability [m^2]
μ viscosity coefficient [Pa·s]
τ time [s]

Abbreviations

IPN   interpenetrating polymer network
LCST   lower critical solution temperature
MBA   N,N′-methylenebisacrylamide
PAAc   poly(acrylic acid)
PAAm   polyacrylamide
PNIPAAm   poly(N-isopropylacrylamide)
SCHL   structural changes in hydration layers
SR   Schopper-Riegler
TRHRS   thermo-responsive hydrated reticular systems (macro-, micro- and sub micro-)
UCST   upper critical solution temperature
UF   urea-formaldehyde

REFERENCES

[1] M. Milichovský, *J. Biomater. Nanobiotechnol.*, **1**, 17 (2010).
[2] L. Martín, M. Alonso, A. Girotti, F. J. Arias and J. C. Rodríguez-Cabello, *Biomacromolecules*, **10**, 3015 (2009).
[3] A. Girotti, J. C. Reguera, F. J. Rodríguez-Cabello, M. Arias, A. Alonso *et al.*, *J. Mater. Sci.: Mater. Med.*, **15**, 479 (2004).
[4] J. E. Wong, A. K. Gaharvar, D. Müller-Schulte, D. Bahadur and W. Richtering, *J. Colloid Interface Sci.*, **324**, 47 (2008).
[5] K. L. Fujimoto, Ma Zuwei, D. M. Nelson, R. Hashizume, J. Guan *et al.*, *Biomaterials*, **30**, 4357 (2009).
[6] J. Xiao-Jie, C. Liang-Yin, L. Li, M. Peng and M. L. Young, *J. Phys. Chem.* B, **112**, 1112 (2008).
[7] J. J. Kang Derwent and W. F. Mieler, *Trans. Am. Ophthalmol. Soc.*, **106**, 206 (2008).

8   Y. H. Bae, R. Okano, S. Hsu and W. Kim, *Macromol. Chem. Rapid Commun.*, **8**, 481 (1987).

9   D. Ghate and H. F. Edelhause, *Expert Opin. Drug Deliv.*, **3**, 275 (2006).

10   T. Yasukawa, Y. Ogura, H. Kimura, E. Sakurai and Y. Tabata, *Expert Opin. Drug Deliv.*, **3**, 261 (2006).

11   S. E. Stabenfeldt, A. J. García and M. C. LaPlaca, *J. Biomed. Mater. Res. Part A*, **77A**, 718 (2006).

12   K. E. Crompton, J. D. Goud, R. V. Bellamkonda, T. R. Gengenbachm, D. I. Finkelstein *et al.*, *Biomaterials*, **28**, 441 (2007).

13   K. Shanmuganathan, J. R. Capadona, S. J. Rowan and C. Weder, *Appl. Mater. Interface.*, **2**, 165 (2010).

14   F. Xia, H. Ge, Y. Hou, T. Sun, L. Chen *et al.*, *Adv. Mater.*, **19**, 2520 (2007).

15   F. D. Jochum and P. Theato, *Macromolecules*, **42**, 5941 (2009).

16   J.-H. Kang, J. H. Moon, S.-K. Lee, S.-G. Park, S. G. Jang *et al.*, *Adv. Mater.*, **20**, 3061 (2008).

17   J. F. Mano, *Adv. Eng. Mater.*, **10**, 515 (2008).

18   M. Yoshida, R. Langer, A. Lendlein and J. Lahan, *J. Macromol. Sci. Polym. Rev.*, **46**, 347 (2006).

19   G. Santaneel, N. Arup, Y. Chao, C. Tong, S. Ghosh Mitra, *et al.*, in *Mater. Res. Soc. Symp. Proc. "Responsive Biomaterials for Biomedical Applications"*, edited by J. Cheng, A. Khademhosseini, H.-Q. Mao, M. Stevens and C. Wang, Warrendale, Pennsylvania, April 2008, vol. 1095, 1095-EE03-20.

20   D. J. Beebe, J. S. Moore, J. M. Bauer, Q. Yu, R. H. Liu *et al.*, *Nature*, **404**, 588 (2000).

21   N. Idota, A. Kikuchi, J. Kobayashi, K. Sakai and T. Okano, *Adv. Mater.*, **17**, 2723 (2005).

22   H. Yang, Y.-H. Han, X.-W. Zhao, K. Nagai and Z.-Z. Gu, *Appl. Phys. Lett.*, **89**, 111 (2006).

23   D. Chandra, J. A. Taylor and S. Yang, *Soft Matter*, **4**, 979 (2008).

24   M. E. Harmon, M. Tang and C. W. Frank, *Polymer*, **44**, 4547 (2003).

25   J. Kim, S. Yun and Z. Ounaies, *Macromolecules*, **39**, 4202 (2006).

26   P. M. Mendes, *Chem. Soc. Rev.*, **37**, 2512 (2008).

27   M. Lutecki, B. Strachotová, M. Uchman, J. Brus, J. Pleštil *et al.*, *Polym. J.*, **38**, 527 (2006).

28   X.-Z. Zhang, F.-J. Wang and Ch.-Ch. Chu, *J. Mater. Sci.: Mater. Med.*, **14**, 451 (2003).

29   H. Hou, W. Kim, M. Grunlan and A. Han, *J. Micromech. Microeng.*, **19**, 1 (2009).

30   R. M. P. da Silva, J. F. Mano and R. L. Reis, *Trends Biotechnol.*, **25**, 577 (2006).

31   H. Hatakeyma, A. Kichuchi, M. Yamato and T. Okano, *Biomaterials*, **27**, 5069 (2006).

32   X.-C. Xiao, L.-Y. Chu, W.-M. Chen and J.-H. Zhu, *Polymer*, **46**, 3199 (2005).

33   R. Yoshida, *Adv. Mater.*, **20**, 1 (2010).

34   K. Edelmann, "Lehrbuch der Kolloidchemie. Band I.", VEB Deutscher Verlag der Wissenschaften, Berlin, 1962.

35   M. Milichovský, *Sb. Věd. Prací, Vys. Škola Chem. Technol., Pardubice*, **56**, 155 (1992/93).

36   M. Milichovský, *Tappi J.*, **73**, 221 (1990).

37   M. Milichovský, *Cellulose Chem. Technol.*, **26**, 607 (1992).

38   M. Milichovský, *Chem. Listy*, **94**, 875 (2000).

39   M. Milichovský, *Pap. Celul.*, **33**, V61 (1978).

40   M. Milichovský and B. Ček, *Cellulose Chem. Technol.*, **38**, 385 (2004).

41   M. Fišerová, J. Gigac and J. Balberčák, *Pap. Celul.*, **64**, 362 (2009).

42   M. Milichovský, *Sb. Věd. Prací, Vys. Škola Chem. Technol., Pardubice*, **56**, 123 (1992/93).

43   M. Milichovský, *Sb. Věd. Prací, Vys. Škola Chem. Technol., Pardubice*, **51**, 149 (1988).

44   M. Milichovský, *Pap. Celul.*, **51**, 61 (1996).